Estimation of a time-varying sea-surface profile for receiver-side de-ghosting

Rob Telling and Sergio Grion*
Shearwater Geoservices, UK

Summary

The presence of a rough sea-surface during acquisition of marine seismic data leads to time- and space-dependent perturbations in the timing of the ghost at the receivers relative to the primary. If not taken into account during de-ghosting, the timing errors can lead to undesirable artefacts in the data. In previous work we and other authors have shown it is possible to correct for these perturbations via explicitly incorporating a snapshot of the sea-surface profile into the ghost model. In this work we derive surfaces from the very low-frequency signal recorded at the streamer. This signal can be related directly to the wave-height and captures the change in the sea-surface profile over the duration of the shot record, therefore enabling time-dependent de-ghosting.

Introduction

Sea-surface profiles derived for rough-sea de-ghosting are typically deduced from the observed frequency of the ghost notch taken from an *f-x* spectrum in a window around a particular event (King et al. 2015, Hardwick et al. 2015, Grion et al. 2016). The difference between the actual notch frequency and that expected for a flat sea surface can be attributed directly to the path length change due to the wave-height above the streamer. This method can only provide a snapshot of the surface at the time of the event and furthermore the interference is only apparent when there are no strong interfering reflections or diffractions present. Typically, events that can be used for this purpose include deep water sea-bottom reflections and their multiples. While de-ghosting may be successful at the time of the selected event, there is no guarantee of the same quality at other times.

In earlier work (Telling and Grion, 2016) we compared sea-surface profiles derived from a 3D shot record via ghost interference and via low-frequency signal and used these to de-ghost the data. We found generally good correlation between surfaces and in both cases there was uplift in de-ghosting quality when comparing to a flat-sea assumption. The ghost interference method gave the greatest improvement at the event from which it is derived but the low-frequency method had the advantage that it could be derived at any time and place in the shot record.

Method

The low frequency signal in the raw data may be used to infer wave height using the linear theory of deep-water surface waves (Kinsman 1965). Cavaleri (1980) discusses estimation of wave height using pressure recordings at a depth below the surface and Kragh and co-authors (2002, 2004, 2006) applied this method to a seismic streamer spread composed of many hydrophones.

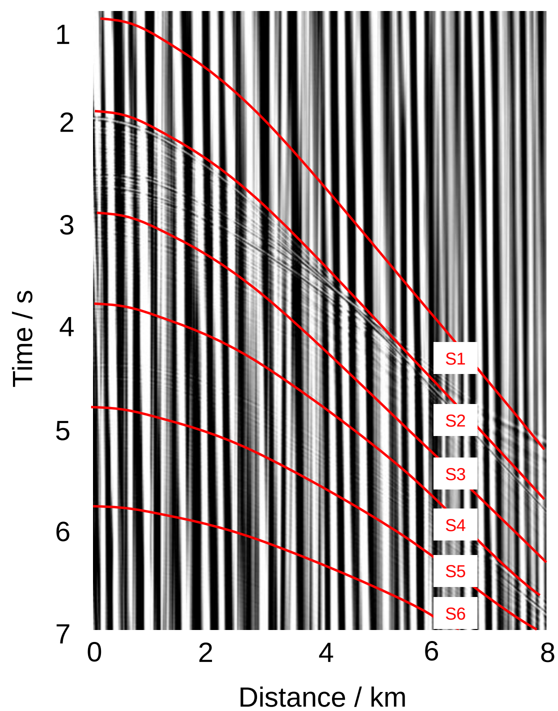

Figure 1 – Example raw shot record showing the dominant low-frequency swell *signal* together with the seismic signal. The red lines denote hyperbolic trajectories for which sea-surfaces are later derived. The two-way time in milliseconds at zero offset are respectively 820 (S1), 1820 (S2), 2820 (S3), 3820 (S4), 4820 (S5) and 5820 (S6).

The departure from mean hydrostatic pressure that is measured at the hydrophone due to the presence of a wave overhead (ignoring the constant components due to cyclical *x* and *z* particle velocities and translational *x* particle velocity) is given by:

$$\Delta p = \rho g S_z e^{-kz} \cos(kx - \omega t) \quad , \qquad (1)$$

where k is the wavenumber, $k = \omega^2/g$ (using the dispersion relation for deep water waves), z is the depth below the mean sea-level of the hydrophone and S_z is the amplitude of the sea-surface wave height. The recorded pressure due to the surface waves decreases exponentially with depth and will decay more rapidly for larger k (smaller wavelengths), so although it is possible to unwrap $S_z(\omega)$ from the measured Δp data using equation 1, we will reach the noise floor more quickly for short wavelengths and deep cables. To sample the low frequency signal properly it is important to use a long time record e.g. concatenating a few shot records made from a continuous recording. One part of a raw shot record showing the nature of this signal is shown in Figure 1 and the *f-k* spectrum of a set of three records, totaling around 30 seconds, is shown in Figure 2. Note the peak energy around 0.08Hz and wavenumber 0.02m^{-1}, corresponding to a wavelength around 300m.

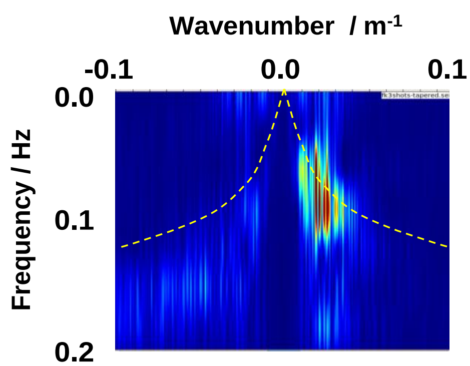

Figure 2 – *f-k* spectrum of 3 concatenated shot records. The annotated yellow lines show the physical limit of the dispersion relation for deep water gravity waves, $\omega^2=gk$.

Once we have derived the sea-surface profile we de-ghost the data using the phase-shift de-ghosting algorithm described in Grion *et al.* (2015), inverting for the up-going wave-field while explicitly handling the variable depth streamer, variable surface profile and irregular offset sampling.

Data example

The data shown here are taken from one streamer (cross-line offset 375m) of a 3D acquisition with 648 grouped channels, 12.5m group spacing and with receiver depth slanting linearly over the interval 12-28m. The Observer's logs report the sea-state as having significant wave-height 2.0 m and wind speed in the range 15-18 knots E to SE. The ship's course was approximately 5knots on a bearing 270° and thus was headed more-or-less with the wind. To sample the low-frequency signal we use a rolling gather of three consecutive shot records at a time, corresponding to 30s duration. Receiver motion correction was applied and the 2Hz analogue first-order high-pass backed-off assuming inverse high-pass transfer function H given by equation 2:

$$H(\omega)^{-1} = \frac{1 + i\omega/\omega_0}{i\omega/\omega_0} \quad , \qquad (2)$$

where ω_0 is the angular frequency at cut-off. We convert voltage measured at the hydrophone to pressure via the nominal hydrophone sensitivity 19.73 V/bar. We then derive surfaces via rearrangement and application of equation 1 as a filter. The time for extracting the surface was chosen along hyperbolic trajectories as indicated in Figure 1 and resulting plots of amplitude versus distance along the streamer are shown in Figure 4.

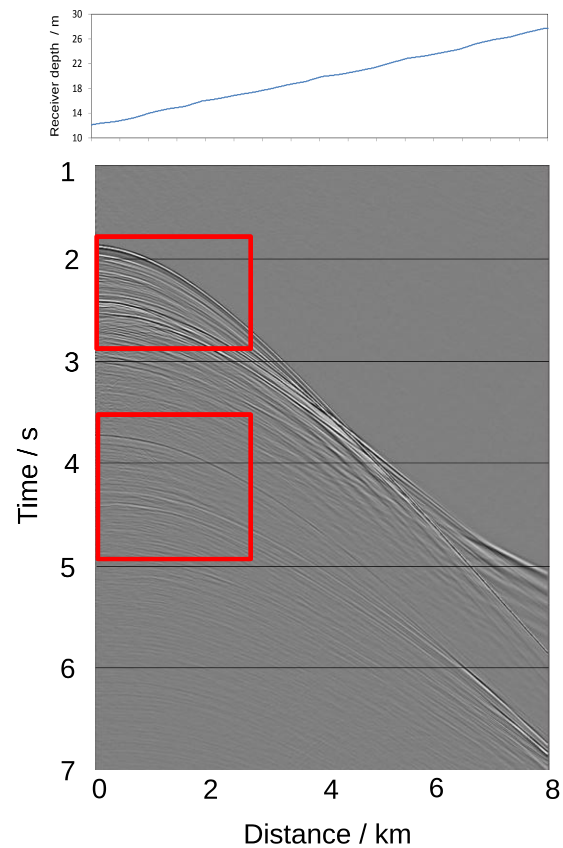

Figure 3 – Shot gather after low-cut filtering prepared as input for de-ghosting. The red boxes show zooms used to display the later results. Above there is a plot of the variation in receiver depth along the length of the streamer.

The data were then de-ghosted firstly in a shallow window then in a deeper window. For the shallow window we de-ghosted the data using a surface derived close to the seabed two-way reflection time (hyperbolic trajectory, zero-offset

1820 ms). For the deeper window we de-ghosted the data using a surface derived close to the time of deep window (hyperbolic trajectory, zero-offset 3820 ms) and also using the surface derived at the earlier time. The objective was to assess the utility of using a time-varying sequence of surfaces in the de-ghosting process. In a final step, we applied a rank-reduction filter to attenuate residual noise.

Results

Figure 4 shows the surfaces derived along the trajectories indicated in Figure 1. There are clearly gross features that appear to be present in each profile but which have evolved and translated along the streamer at each subsequent time. Note that as the ship was travelling with the wind and also thus presumably with the predominant surface wave direction we will not expect changes over time as great as if the ship were travelling in the opposite direction. We see from Figure 5 that there is an improvement in data quality after de-ghosting when using an explicit sea-surface profile versus the flat-sea assumption. Figure 6 then shows the result of assuming a frozen shallow sea-surface (the same surface as derived for the de-ghosting in Figure 5) and the result if we use a surface derived closest to the deep window. Again, there is benefit in doing so, in terms of number and strength of artefacts and in fact there is evidence here to suggest that de-ghosting with the wrong surface is even worse than assuming a flat sea-surface.

The achieved results demonstrate that a time varying sea-surface can bring benefits to de-ghosting quality. The example shown relates to two distinct time-space windows of about 1 second in length. A natural question is then if a truly sample-by-sample time-variant de-ghosting would be feasible. We think the answer is yes, but we have not explored this route so far. There are two main reasons for this choice: The first is that this would add extra dimensions (and substantial computational cost) to the phase-shift de-ghosting operator described by Grion et al. 2016; The second is that the use of variable-depth streamers and sea surfaces derived at discrete intervals leaves, in our experience, small, spatially un-correlated artefacts in the presence of a rough sea, and these can be effectively removed by random noise attenuation, as shown in figures 5 and 6. We successfully used a rank-reduction filter (Trickett et al. 2012) for this purpose.

Conclusions

It is striking that 0.1 Hz swell signal can be recovered from towed streamer data. In past work we have shown that sea surfaces estimated using seismic events and using swell signal are largely in agreement, a confirmation that these estimations have physical meaning. In the present work we use time-variant sea-surface profiles in receiver-side de-ghosting, and show that there is a noticeable improvement when events are de-ghosted using a sea-surface corresponding to their travel-time. Note that in this study the ship's course is aligned with the wave direction and therefore evolution of the sea-surface with time is not at its greatest. The importance of including time-variance may indeed be greater for an opposing or inclined wave direction.

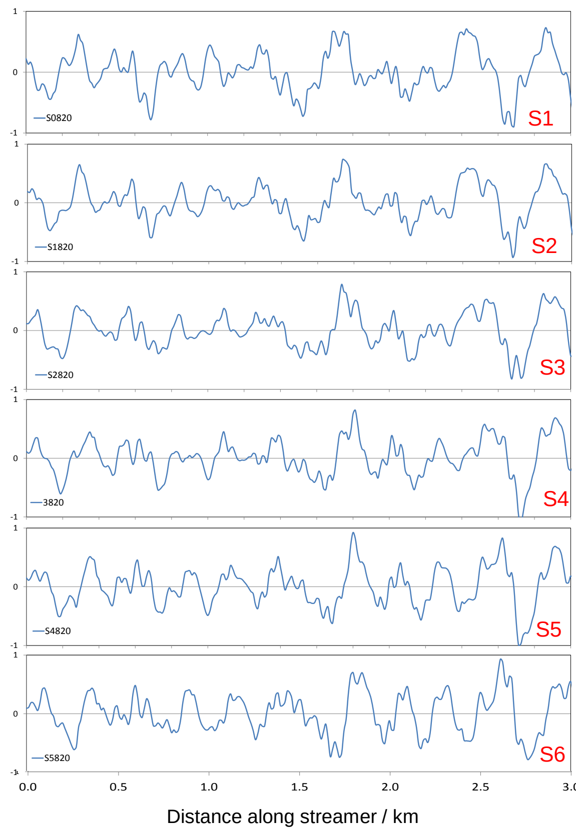

Figure 4 – A sequence of sea-surface profiles derived along the streamer from the low-frequency signal at 1 s intervals of the zero-offset start-time and along hyperbolic trajectories as shown in the example shot record in Figure 1. The vertical axis is surface wave amplitude, full-scale ±1 m.

The inclusion of estimated sea-surfaces in the de-ghosting operator improves their accuracy, and therefore reduces the need for stabilising damping factors or statistical representations of the sea surface. These can impose phase and amplitude distortions on the data, and should be avoided whenever possible. Any remaining post-de-ghosting artefacts appear spatially uncorrelated after our rough-sea de-ghosting, and can be attenuated using a random noise attenuator.

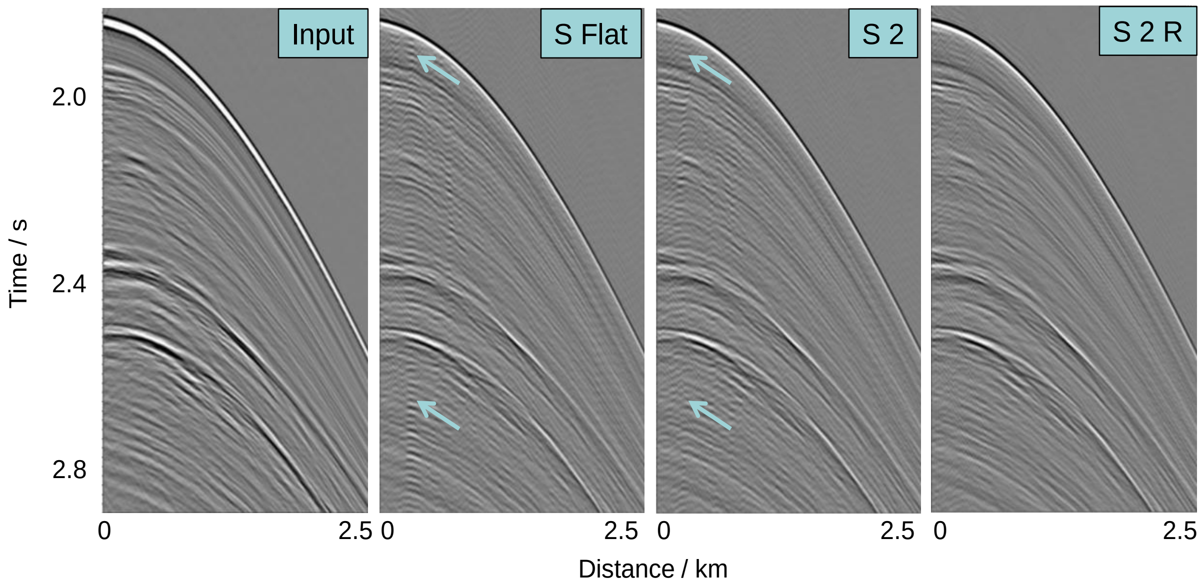

Figure 5 – Shallow window de-ghosting results. From left to right: data prior to de-ghosting (Input), de-ghosted data where it is assumed the sea-surface is flat (S flat), de-ghosted data using the surface profile closest to the sea-bed two-way-time (S2) and finally the data which is the S2 surface result with a rank-reduction filter applied to attenuate the random noise level raised by the de-ghosting operation (S2R).

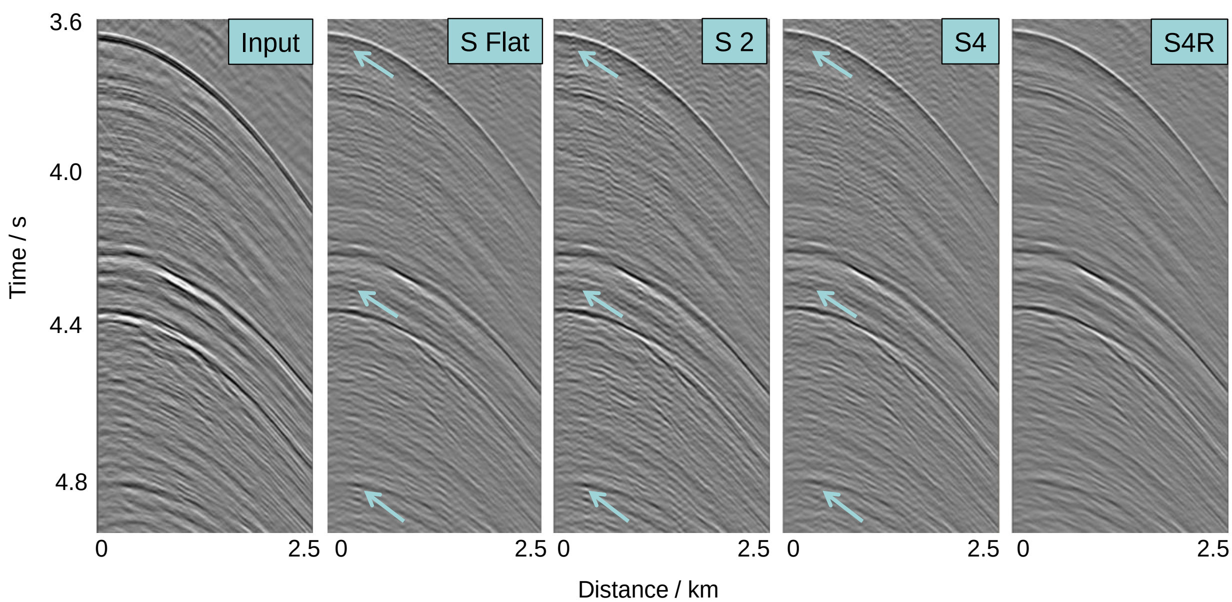

Figure 6 - Deep window de-ghosting results. From left to right: data prior to de-ghosting (Input), de-ghosted data where it is assumed the sea-surface is flat (S flat), de-ghosted data using the surface profile closest to the sea-bed two-way-time (S2) as in Figure 5, de-ghosted data using the surface derived closest to the actual data time window (S4) and finally the result with the S4 surface with a rank-reduction filter applied to attenuate random noise level raised by the de-ghosting operation (S4R).

References

Cavaleri, L., 1980, Wave measurement using pressure transducer, Oceanologica Acta, 3(3)

Grion, S., Telling, R., and S. Holland, 2016, Rough sea estimation for phase-shift de-ghosting: 86th Annual SEG Meeting Expanded Abstracts, 5129-5133

Hardwick, A., Charron, P., Masoomzadeh, H., Aiyepeku, A., Cox, P. and S. Laha, 2015, Accounting for sea surface variation in deghosting – a novel approach applied to a 3D dataset offshore West Africa: 85th Annual SEG Meeting Expanded Abstracts, 4615-4619

King, S. and G. Poole, 2015, Hydrophone-only receiver deghosting using a variable sea surface datum: 85th Annual SEG Meeting Expanded Abstracts, 4610-4614

Kinsman B., 1965, Wind Waves. Prentice-Hall Inc., Englewood, Cliffs, New Jersey

Kragh, E., Laws, R. and L. Combee, 2002, Sea-surface shape derivation above the seismic streamer: 64th EAGE Conference, Extended Abstracts, A-07

Kragh, E., Robertsson, J., Laws, R., Amundsen, L., Rosten, T., Davies, T., Zerouk, K. and A. Strudley, , 2004, Rough-sea deghosting using wave-heights derived from low-frequency pressure recordings– A case study: 74th Annual SEG Meeting, Expanded Abstracts, 1309-1312

Laws, R. and E. Kragh, 2006, Sea surface shape derivation above the seismic streamer, Geophysical Prospecting, 54, 817-828

Telling, R. H. and S. Grion, 2016, Comparison of methods for rough sea-surface estimation: 79th EAGE Conference, Extended Abstracts, We P5 11

Trickett, S., Burroughs, L. and A. Milton, 2012, Robust rank-reduction filtering for erratic noise:.82nd Annual SEG Meeting Expanded Abstracts, 1-5.